A Sliding Mode Controller based on Backstepping for Manipulator

Haitao Zhang, Xiaofeng Liu, and Guifang Wu

Abstract—**Based on two-joint rigid manipulator, we analyze its kinematics and dynamics, establish forward and inverse kinematic model of the manipulator, and plan the joint trajectory using the high order polynomial interpolation method. Then utilizing dynamic equation established by Lagrange equation, we propose a sliding mode control method based on linear sliding surface and backstepping, use adaptive method to estimate the uncertainty from external disturbances, and prove the system stability based on Lyapunov theory. After the dual power reaching law and terminal sliding surface are further used instead of power reaching law and linear sliding surface, the initial torque become much smaller. Finally the lower torque limit of the first link is set up so as to further lessen initial torque, accelerate the tracking speed, and adapt to practical engineering requirements. The simulation results show the validity of the proposed method.**

Index Terms—**kinematics, backstepping, sliding mode, Lyapunov**

I. Introduction

With the development of modern industry, the automation of manufacturing industry has become an inevitable direction, which makes the manipulator extensively used in the machining industry with its own remarkable characteristics. The effective application of manipulator has greatly improved the production efficiency. In order to further improve the automation level of machining industry, it is very important to study more advanced control method of the manipulator.

For the study of the manipulator kinematics, the classical D-H method can be used to establish the kinematic model of the manipulator, and the inverse kinematics can also be solved by using forward kinematics. When the manipulator performs the limited operation, its trajectory needs to be planned and coordinated. Currently many scholars have done a lot of theoretical research in this area. Yiwei Zhang [1] used high order polynomial to do the trajectory planning of the robot. Zhong Shi [2] used high order polynomial and particle swarm optimization algorithm to solve the planning problem, and the simulation results verify the feasibility of the algorithm.

Sliding mode control is a kind of variable structure control with strong robustness. The control method can make the system state slide along the sliding surface by switching the control amount and keep stable under parameter perturbation and external disturbance. Because of this characteristic, the sliding mode control has been applied in robot control [3]–[6]. Hong Mei [7] proposed a dual power reaching law which combines with the sliding surface, and get better control effect. Wenhui Zhang [8] used a neural network control scheme with sliding mode variable structure. The system also has good control effect in the case of strong interference. Kewen Tong [9] adopted the integral sliding surface and continuous function to reduce chattering. Chunshan Xu [10] designed a fast terminal sliding surface combined the smooth index reaching law, and discussed the convergence domain.

Backstepping control method has a better effect in the realization of uncertain systems, especially when the interference or uncertainty does not meet the matching conditions. The basic idea of the backstepping control is to decompose the complex nonlinear system into subsystems which do not exceed the order of systems until the design of the control law is completed [11]. Chuanzhong Xu [12] designed the sliding mode controller considering modeling errors. The neural network is used to estimate the modeling errors, and the better simulation results are obtained.

In this paper, we first analyze the kinematics and dynamics of the manipulator, establish forward and inverse kinematic model of the manipulator, and plan the joint trajectory using the high order polynomial interpolation method. Then utilizing dynamic equation established by Lagrange equation, we propose a sliding mode control method based on backstepping and linear sliding surface, use adaptive method to estimate the uncertainty from external disturbances, and prove the system stability based on Lyapunov theory. Then aimed at the deficiency of the larger initial torque, the dual power reaching law and terminal sliding surface are used to reduce the initial torque. Finally the lower torque limit of the first link is set up to further lessen initial torque and accelerate the tracking speed.

II. Trajectory of Manipulator

A. Kinematics Analysis of Manipulator

Utilizing kinematics analysis of the manipulator, we can get the transformation matrix of the end position with respect to the origin of the manipulator system. And utilizing inverse kinematic analysis, the joint variables can be obtained by the end position. In this paper, we use modified D-H modeling

Manuscript received February 7, 2017; revised April 8, 2017. This work was supported in part by the key scientific research project of universities and colleges of Henan Province under Grant 15A413003.

Haitao Zhang is with the Information Engineering College, Henan University of Science and Technology, Luoyang, CO 471023 China (corresponding author: e-mail: zhang_haitao@163.com).

XiaoFeng Liu is with the Information Engineering College, Henan University of Science and Technology, Luoyang, CO 471023 China.

Guifang Wu is with the Information Engineering College, Henan University of Science and Technology, Luoyang, CO 471023 China.

method for two-joint rigid manipulator. The modified D-H method requires a coordinate system for all the joints of the manipulator. In general, the base coordinate frame is first established. Then the coordinate frame of each link is respectively established. Fig. 1 is the coordinate system of two-joint rigid manipulator.

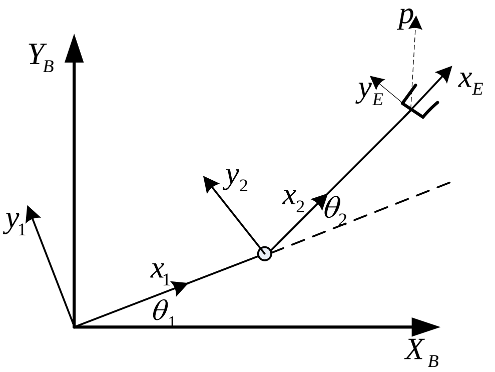

Fig. 1. The link coordinate system of manipulator

In Fig. 1, the letter *B* represents the base coordinates, letter *E* represents the end coordinates, and letter *p* is a point in the end coordinate system. According to homogeneous transformation, we can get the position and orientation of the manipulator.

$$\left.\begin{array}{ll}
\begin{bmatrix} {}^{B}p \\ 1 \end{bmatrix} = {}^{B}T_{\mathrm{E}} \begin{bmatrix} {}^{\mathrm{E}}p \\ 1 \end{bmatrix} & {}^{B}T_{E} = \begin{bmatrix} {}^{B}R_{E} & {}^{B}P_{E} \\ 0^{T} & 1 \end{bmatrix} \\
\begin{bmatrix} {}^{B}p \\ 1 \end{bmatrix} = {}^{B}T_{1} \begin{bmatrix} {}^{1}p_{p} \\ 1 \end{bmatrix} & {}^{B}T_{1} = \begin{bmatrix} {}^{B}R_{1} & {}^{B}P_{1} \\ 0^{T} & 1 \end{bmatrix} \\
\begin{bmatrix} {}^{1}p \\ 1 \end{bmatrix} = {}^{1}T_{2} \begin{bmatrix} {}^{2}p \\ 1 \end{bmatrix} & {}^{1}T_{2} = \begin{bmatrix} {}^{1}R_{2} & {}^{1}P_{2} \\ 0^{T} & 1 \end{bmatrix} \\
\begin{bmatrix} {}^{2}p \\ 1 \end{bmatrix} = {}^{2}T_{E} \begin{bmatrix} {}^{E}p \\ 1 \end{bmatrix} & {}^{2}T_{E} = \begin{bmatrix} {}^{2}R_{\mathrm{E}} & {}^{1}P_{\mathrm{E}} \\ 0^{T} & 1 \end{bmatrix}
\end{array}\right\} \tag{1}$$

So we may get:

$$ {}^{B}T_{E} = {}^{B}T_{1}\,{}^{1}T_{2}\,{}^{2}T_{E} \tag{2}$$

It can be seen from the Fig. 1, the coordinate frame 1 has no translation, and just rotates θ_1 with respect to the base frame; the coordinate frame 2 translates l_1 and rotates θ_2 with respect to the coordinate frame 1; the coordinate frame *E* of the end effector just translates l_2 with respect to the coordinate frame 2. Therefore, we may get:

$$\left.\begin{array}{l}
{}^{B}p_{1} = \begin{bmatrix} 0 \\ 0 \end{bmatrix} \\
{}^{B}R_{1} = \begin{bmatrix} \cos\theta_1 & -\sin\theta_1 \\ \sin\theta_1 & \cos\theta_1 \end{bmatrix} \\
{}^{1}p_{2} = \begin{bmatrix} l_1 \\ 0 \end{bmatrix} \\
{}^{1}R_{2} = \begin{bmatrix} \cos\theta_2 & -\sin\theta_2 \\ \sin\theta_2 & \cos\theta_2 \end{bmatrix} \\
{}^{2}p_{E} = \begin{bmatrix} l_2 \\ 0 \end{bmatrix} \\
{}^{2}R_{E} = \begin{bmatrix} 1 & 0 \\ 0 & 1 \end{bmatrix}
\end{array}\right\} \tag{3}$$

Homogeneous transformation matrix of each joint can be shown as follows.

$$\left.\begin{array}{l}
{}^{B}T_{1} = \begin{bmatrix} \cos\theta_1 & -\sin\theta_1 & 0 \\ \sin\theta_1 & \cos\theta_1 & 0 \\ 0 & 0 & 1 \end{bmatrix} \\
{}^{1}T_{2} = \begin{bmatrix} \cos\theta_2 & -\sin\theta_2 & l_1 \\ \sin\theta_2 & \cos\theta_2 & 0 \\ 0 & 0 & 1 \end{bmatrix} \\
{}^{2}T_{E} = \begin{bmatrix} 1 & 0 & l_2 \\ 0 & 1 & 0 \\ 0 & 0 & 1 \end{bmatrix}
\end{array}\right\} \tag{4}$$

In general, from the Equation (1), (2), (3) and (4), the final homogeneous transformation matrix can be shown as follows.

$$ {}^{B}T_{E} = \begin{bmatrix} \cos(\theta_1+\theta_2) & -\sin(\theta_1+\theta_2) & l_1\cos\theta_1 + l_2\cos(\theta_1+\theta_2) \\ \sin(\theta_1+\theta_2) & -\cos(\theta_1+\theta_2) & l_1\sin\theta_1 + l_2\sin(\theta_1+\theta_2) \\ 0 & 0 & 1 \end{bmatrix} \tag{5}$$

Assuming that the point *p* is located in the frame of end effector, the forward kinematics solution of the point *p* may be obtained.

$$ p=\begin{bmatrix} x \\ y \end{bmatrix}, \theta=\begin{bmatrix} \theta_1 \\ \theta_2 \end{bmatrix} \tag{6}$$

$$\left.\begin{array}{l} x = l_1\cos\theta_1 + l_2\cos(\theta_1+\theta_2) \\ \mathrm{y} = l_1\sin\theta_1 + l_2\sin(\theta_1+\theta_2) \end{array}\right\} \tag{7}$$

In the analysis and design of manipulator, the solution of inverse kinematics is very important. Usually the control of the manipulator is to make the manipulator reach the desired position, which needs each joint angle to be determined so as to achieve the specified position. Each joint angle is obtained by solving the inverse kinematics equation.

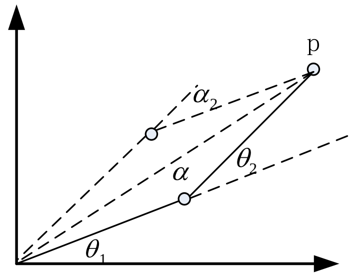

Fig. 2. The two trajectory of manipulator

The position of end effector is known, and we may solve the joint angles by the following equation.

$$\theta=f^{-1}(\mathrm{p}) \tag{8}$$

From Fig. 2 we may get:

$$\theta_2=\pi-\alpha \tag{9}$$

According to cosine formula, we may get:

$$\cos\alpha=\frac{l_1^2+l_2^2-(x^2+y^2)}{2l_1l_2} \tag{10}$$

So we get:

$$\theta_1=\tan^{-1}(\frac{y}{x})-\tan^{-1}(\frac{l_2\sin\theta_2}{l_1+l_2\cos\theta_2}) \tag{11}$$

Utilizing the above equations, the joint angles can be obtained. In fact, two groups of solutions are gotten by using inverse kinematics for two-freedom-degree manipulator. As shown in Fig.2, we discard a set of data which is represented by dashed line, and use another group to solve the following questions.

B. *Polynomial Interpolation*

In order to control the motion of the manipulator in the joint space, the position of the joint should be calculated by interpolation. For the starting position and the target position of the joint space, the middle position of the joint can be calculated by interpolation. In this paper, we use the five order polynomial to calculate the desired joint position of each trajectory point. Assuming that the joint position in the t_0 and t_f time are q_0 and q_f, the velocity of joint movement are $\dot{q}_0$ and $\dot{q}_f$, and the acceleration are $\ddot{q}_0$ and $\ddot{q}_f$. So we can get the boundary conditions of the joint movement of the manipulator.

$$\begin{cases} q(0)=q_0, q(t_f)=q_f \\ \dot{q}(0)=\dot{q}_0, \dot{q}(t_f)=\dot{q}_f \\ \ddot{q}(0)=\ddot{q}_0, \ddot{q}(t_f)=\ddot{q}_f \end{cases} \tag{12}$$

Because Equation (12) has 6 conditions, so the high order polynomial may have 6 coefficients. The joint position is represented by Equation (13) of the five order polynomial, and the joint velocity and acceleration may be obtained by the derivative.

$$q(t)=a_0+a_1t+a_2t^2+a_3t^3+a_4t^4+a_5t^5 \tag{13}$$

$$\begin{cases} \dot{q}(t)=a_1+2a_2t+3a_3t^2+4a_4t^3+5a_5t^4 \\ \ddot{q}(t)=2a_2+6a_3t+12a_4t^2+20a_5t^3 \end{cases} \tag{14}$$

By solving (12), (13) and (14), the coefficients a_0, a_1, a_2, a_3, a_4 and a_5 can be gotten.

$$\begin{cases} a_0=q_0 \\ a_1=\dot{q}_0 \\ a_2=\dfrac{\ddot{q}_0}{2} \\ a_3=\dfrac{20q_{f-}20q_0-(8\dot{q}_f+12\dot{q}_0)t_f-(3\ddot{q}_0-\ddot{q}_f)t_f^2}{2t_f^3} \\ a_4=\dfrac{-30q_f+30q_0+(14\dot{q}_f+16\dot{q}_0)t_f+(3\ddot{q}_0-2\ddot{q}_f)t_f^2}{2t_f^4} \\ a_5=\dfrac{12q_f-12q_0-(6\dot{q}_f+6\dot{q}_0)t_f-(\ddot{q}_0-\ddot{q}_f)t_f^2}{2t_f^5} \end{cases} \tag{15}$$

Suppose the initial joint angles are both 0, the final joint angles are respectively 1 and 0.5, the running time of the system is 10s, and the functions of two joint angles are:

$$\begin{cases} \theta_1(\mathrm{t})=\dfrac{3}{50000}t^5-\dfrac{3}{2000}t^4+\dfrac{1}{100}t^3 \\ \theta_2(\mathrm{t})=\dfrac{3}{100000}t^5-\dfrac{3}{4000}t^4+\dfrac{1}{200}t^3 \end{cases} \tag{16}$$

III. Design of Backstepping Sliding Mode Controller

A. *State Equation of Manipulator*

Regardless of model error, Lagrange dynamics equation is as follows.

$$M(q)\ddot{q}+C(q,q)\dot{q}+G(q)=\tau+\tau_d \tag{17}$$

where, M is the symmetric positive definite inertia matrix, C is the vector matrix containing Coriolis and centrifugal force, and G is the gravity vector matrix. q, $\dot{q}$ and $\ddot{q}$ are the position vector, the velocity vector and the acceleration vector. τ is the input torque , and τ_d is external disturbance.

Suppose that $x_1=q, x_2=\dot{q}$. Equation (18) can be gotten from Equation (17).

$$\begin{cases} \dot{x}_1=x_2 \\ \dot{x}_2=M^{-1}(\tau+\tau_d-Cx_2-G) \\ y=x_1 \end{cases} \tag{18}$$

B. *Definition of Variables*

The basic design method of backstepping control is as follows. First, define the state error e_1 and e_2.

$$e_1=x_1-q_d \tag{19}$$

$$e_2=x_2-\alpha_1 \tag{20}$$

In Equation (19), q_d is given joint angles, and α_1 is virtual control quantity.

$$\alpha_1=-k_1e_1+\dot{q}_d \tag{21}$$

Then, we may get:

$$\dot{e}_1=\dot{x}_1-\dot{q}_d=x_2-\dot{q}_d=e_2-k_1e_1 \tag{22}$$

$$\dot{e}_2=\dot{x}_2-\dot{\alpha}_1=M^{-1}(\tau+\tau_d-Cx_2-G)-\ddot{q}_d+k_1\dot{e}_1 \tag{23}$$

Defining the sliding surface switching function:

$$s=ce_1+e_2 \tag{24}$$

where, $c>0$.

C. Design of Reaching Law

In order to improve the control performance of sliding control, it is important to eliminate or weaken chattering. A good reaching law can not only weaken the chattering in the system, but also speed up the system sliding time from any initial state to sliding mode surface, and improve the robustness of the system. In this paper, the reaching law is adopted as follows:

$$\dot{s} = -\varepsilon |s|^{a} \operatorname{sgn} s - k_2 s \tag{25}$$

where $\varepsilon > 0$, $k_2 > 0$. This is a combination of the power reaching law and exponential reaching law.

To a certain extent, the continuous function and the sign function may both inhibit the chattering. However, because of the discontinuity of the sign function, as shown in Fig.3, there is a certain chattering in the process of switching. So we use the arctangent function instead of sign function. The arctangent function is represented as follows.

$$\operatorname{sgn} s = 2/\pi \arctan s \tag{26}$$

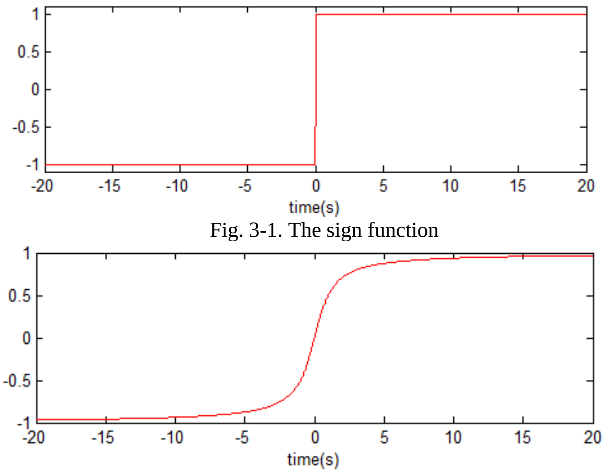

Fig. 3-1. The sign function

Fig. 3-2. $2/\pi \arctan x$ function

Fig.3. The comparison of the continuous function and the sign function

D. Sliding mode controller

Defining the Lyapunov function:

$$v_m = \frac{1}{2} s^2 \tag{27}$$

Then, differentiate Equation (27), we may get:

$$\dot{v}_m = s\dot{s} = -\frac{2\varepsilon}{\pi} s|s|^{a} \arctan s - k_2 s^2 \tag{28}$$

From Equation (28), we may know that when $s > 0$, $\arctan s > 0$; when $s < 0$, $\arctan s < 0$; whatever s is, $-s \arctan s \le 0$. So $\dot{v}_m \le 0$ is always correct, and the system can reach the sliding mode face in finite time.

The input torque is:

$$\begin{aligned} \tau = &-Mc_1(e_2 - k_1 e_1) + C(e_2 + \alpha_1) + G + \\ &M(\ddot{q}_d - k_1 e_1 - \varepsilon |s|^{a} \operatorname{sgn} s - k_2 s) - \tau_d \end{aligned} \tag{29}$$

E. Design of Backstepping Controller

In the following, we use the backstepping method to estimate τ_d.

Then letting $\tilde{\tau}_d = \tau_d - \hat{\tau}_d$, $\lambda > 0$, and defining the first lyapunov function:

$$v_1 = \frac{1}{2} e_1^{2} \tag{30}$$

So, we may get:

$$\dot{v}_1 = e_1 \dot{e}_1 = e_1 e_2 - k_1 e_1^{2} \tag{31}$$

Then we define the second Lyapunov function.

$$v = v_1 + \frac{1}{2} s^2 + \frac{1}{2\lambda} \tilde{\tau}_d^2 \tag{32}$$

We may get:

$$\begin{aligned} \dot{v} &= \dot{v}_1 + s\dot{s} - \frac{1}{\lambda} \tilde{\tau}_d (\hat{\tau}_d) \\ &= e_1 e_2 - k_1 e_1^{2} + s(c_1 \dot{e}_1 + \dot{e}_2) - \frac{1}{\lambda} \tilde{\tau}_d (\dot{\hat{\tau}}_d) \\ &= e_1 e_2 - k_1 e_1^{2} + s[c_1 (e_2 - k_1 e_1) + \\ &\quad M^{-1}(\tau + \hat{\tau}_d - Cx_2 - G) + k_1 \dot{e}_1 - \ddot{q}_d] \\ &\quad + \tilde{\tau}_d \left(\frac{s}{M} - \frac{1}{\lambda} \dot{\hat{\tau}}_d\right) \end{aligned} \tag{33}$$

So we may design adaptive law.

$$\dot{\hat{\tau}}_d = M^{-1} s \lambda \tag{34}$$

We substitute Equation (34) into Equation (33), and get:

$$\begin{aligned} \dot{v} &= e_1 e_2 - k_1 e_1^{2} - s\left(\frac{2\varepsilon}{\pi} |s|^{a} \arctan s - k_2 s\right) \\ &= e_1 e_2 - k_1 e_1^{2} + k_2 s^2 - \frac{2\varepsilon}{\pi} |s|^{a}\, s \arctan s \end{aligned} \tag{35}$$

Defining:

$$Q = \begin{bmatrix} k_2 c_1^{2} + k_1 & k_2 c - \frac{1}{2} \\ k_2 c - \frac{1}{2} & k_2 \end{bmatrix} \tag{36}$$

Setting $e^T = [e_1 \quad e_2]$, we may get:

$$\begin{aligned} e^T Q e &= [e_1 \quad e_2] \begin{bmatrix} k_2 c_1^{2} + k_1 & k_2 c - \frac{1}{2} \\ k_2 c - \frac{1}{2} & k_2 \end{bmatrix} \begin{bmatrix} e_1 \\ e_2 \end{bmatrix} \\ &= k_1 e_1^{2} - e_1 e_2 + k_2 s^2 \end{aligned} \tag{37}$$

Substituting Equation (37) into Equation (35), and get:

$$\dot{v} = -e^T Q e - \frac{2\varepsilon}{\pi} |s|^{a}\, s \arctan s \tag{38}$$

And,

$$\begin{aligned} |Q| &= k_2 (k_2 c_1^{2} + k_1) - (k_2 c - \frac{1}{2})^2 \\ &= k_1 k_2 + k_2 c_1 - \frac{1}{4} \end{aligned} \tag{39}$$

So we can choose the values of k_1, k_2 and c_1 to make $|Q| > 0$.

As is shown above, $\dot{v} \le 0$, and the system satisfies the condition of Lyapunov stability theory.

IV. Simulation

A. Simulation Results

In the manipulator dynamics Equation (17), all parameters are as follows:

$$M(q)=\begin{pmatrix} v+q_{01}+2q_{02}\cos q_2 & q_{01}+q_{02}\cos q_2 \\ q_{01}+q_{02}\cos q_2 & q_{01} \end{pmatrix}$$

$$C(q,\dot{q})=\begin{pmatrix} -q_{02}\dot{q}_2\sin q_2 & -q_{02}(\dot{q}_1+\dot{q}_2)\sin q_2 \\ q_{02}\dot{q}_1\sin q_2 & 0 \end{pmatrix}$$

$$G(q)=\begin{pmatrix} q_{03}g\cos q_1+q_{04}g\cos(q_1+q_2) \\ q_{04}g\cos(q_1+q_2) \end{pmatrix}$$

And,

$$v=(m_1+m_2)l_1^{\,2}$$
$$q_{01}=m_2l_2^{\,2}$$
$$q_{02}=m_2l_1l_2$$
$$q_{03}=(m_1+m_2)l_1$$
$$q_{04}=m_2l_2$$

In the manipulator dynamics Equation (17), the parameters are: $m_1=4kg$, $m_2=2kg$, $l_1=1m$, $l_2=0.8m$, $a=1.2$, $k_1=20$, $k_2=25$, $c=\begin{bmatrix}4 & 0\\ 0 & 16\end{bmatrix}$, $\varepsilon=10$, $\lambda=80$.

The desired positions of two joints are Equation (16), the initial state of system is:

$$[q_1 \quad q_2 \quad q_3 \quad q_4]=[0.5 \quad 0.3 \quad -0.5 \quad 0.5]$$

The simulation results of traditional sliding mode controller are in Fig.4. The simulation results of backstepping sliding mode controller are in Fig.5. The results are as follows:

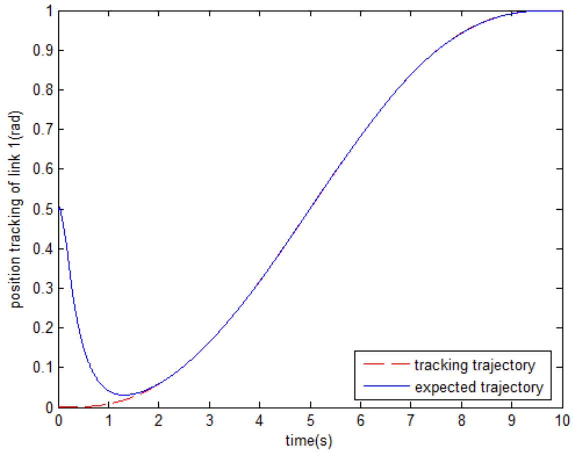

(4-1) The position tracking of link 1

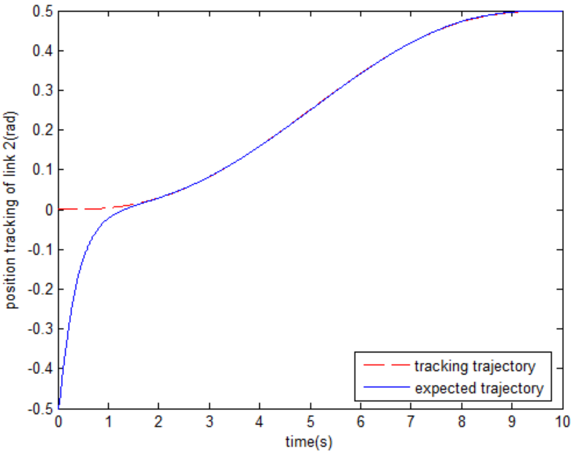

(4-2) The position tracking of link 2

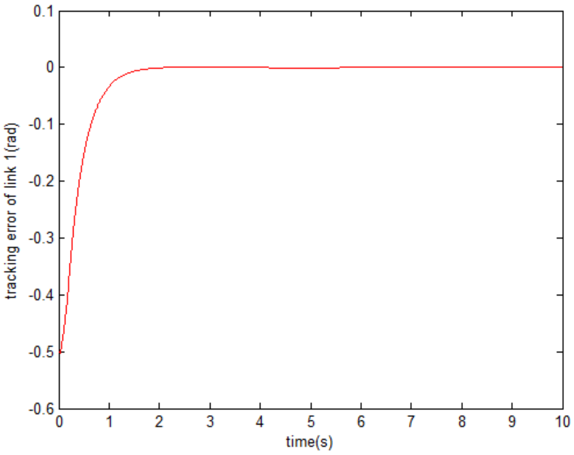

(4-3) The tracking error of link 1

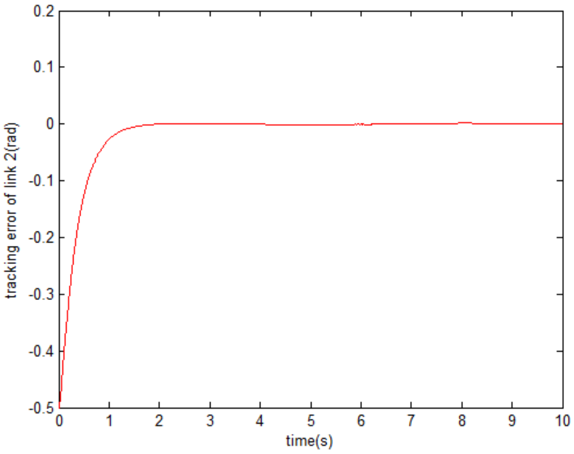

(4-4) The tracking error of link 2

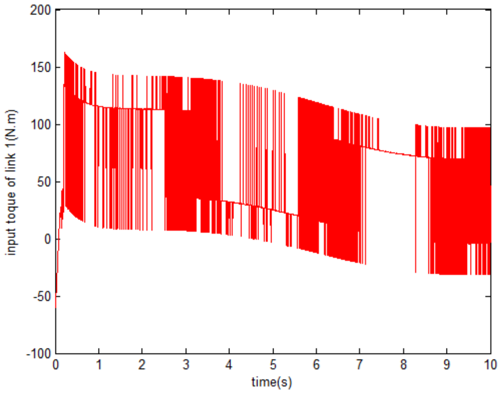

(4-5) The input torque of link 1

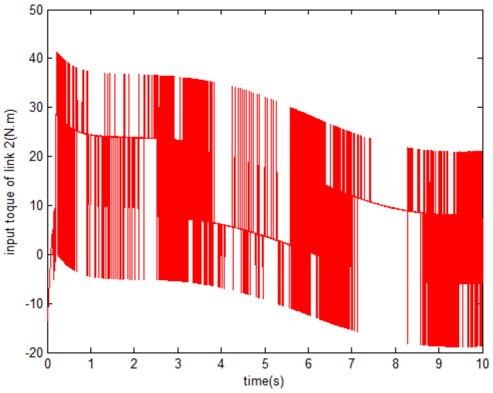

(4-6) The input torque of link 2

Fig. 4. The traditional sliding mode controller simulation diagram

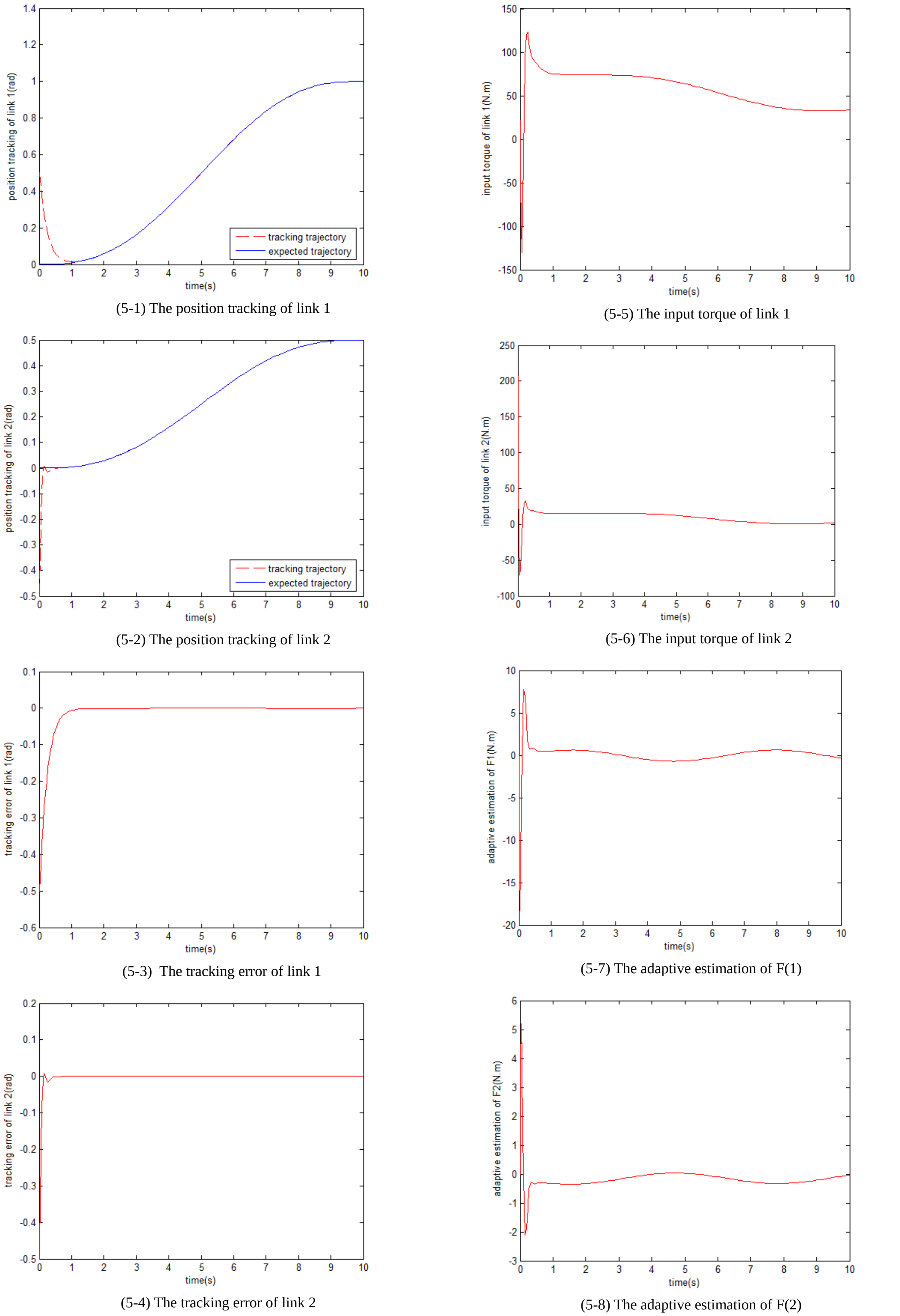

(5-1) The position tracking of link 1

(5-5) The input torque of link 1

(5-2) The position tracking of link 2

(5-6) The input torque of link 2

(5-3) The tracking error of link 1

(5-7) The adaptive estimation of F(1)

(5-4) The tracking error of link 2

(5-8) The adaptive estimation of F(2)

Fig. 5 The improved sliding mode controller using linear sliding surface

We may see from Fig. 4 that the traditional sliding mode controller has a good tracking effect, and can achieve a stable state in a relatively short time. The tracking error of two joints in the initial stage is large, and gradually keeps up with expected angle 1.4s later. Because of external disturbance, we may still see some fluctuations after successful tracking. It may be seen from the control torque that the system appears relatively large fluctuations which shows that the suppression effect to the chattering is not very good. However, it may be seen clearly from Fig. 5, the link 1 takes a second or so to reach the balance state; there are fluctuations in the initial stage of the link 2, but it quickly reaches the balance. For the control torque, there is a relatively large input torque at the beginning stage, and then it becomes stable. Compared with Fig. 4, the control torque curve is smoother, which also means that the reaching law has played a good effect. From the change curve of adaptive parameters of Fig. 5.7 and Fig. 5.8, the estimation of F is relatively ideal.

B. The Simulation Problem and Improved Method

From Fig. 5-5 and Fig. 5-6 we know that the above presented control method needs larger initial torque than normal operating torque. Especially for link 2, the normal operating torque is about 30N.m, but its initial torque needs to reach more than 200N.m. In this situation, In order to improve this problem, we may further improve the proposed method.

In sliding mode control, the reaching law can improve the reaching motion. In Equation (25)，the reaching law includes the power reaching law and the exponential reaching. In order to decrease the chatter of initial torque, the following dual power reaching law can be used [14].

$$\dot{s} = -\varepsilon_1 |s|^a \operatorname{sgn} s - \varepsilon_2 |s|^b \operatorname{sgn} s - k_2 s$$

(40)

where $\varepsilon_1 > 0$, $\varepsilon_2 > 0$, $k_2 > 0$, $a > 1$, and $0 < b < 1$.

No matter the power reaching law or the exponential reaching law, they make the system smoothly reach sliding surface, but they both slow down the speed of reaching sliding surface. So we introduce terminal sliding surface instead of linear sliding surface. The terminal sliding surface can make system reach stable state in limited time, while the linear sliding surface can just make the system reach stable state in unlimited time [15].

The following fast terminal sliding surface is adopted [16].

$$s = ce_1 + e_2 + de_1^{m/n} \tag{41}$$

where $c > 0$, $d > 0$; $m > 0$, $n > 0$, m and n are both odd numbers, and $m < n < 2m$.

C. Simulation of Improved Method

We combine dual power reaching law and fast terminal sliding surface with backstepping, and the related parameters is as follows: $a = 1.2$, $b = 0.8$, $\varepsilon_1 = 0.1$, $\varepsilon_2 = 0.1$, $k_1 = 20$, $k_2 = 25$, $c = \begin{bmatrix} 3 & 0 \\ 0 & 13 \end{bmatrix}$, $d = \begin{bmatrix} 3 \\ 13 \end{bmatrix}$, $m = 0.1$, $n = 0.1$, $\lambda = 80$.

Fig. 6 is the simulation result.

Known from Fig. 6-5 and Fig. 6-6, the initial torque is much smaller compared with Fig. 5-5 and Fig. 5-6. But this effect is obtained by slowing down the response speed. Seen from Fig. 6-1 to Fig. 6-4, the time of following expected trajectory has increased by about 0.2s. However, a small reduction of response speed is worthwhile for the performance improvement of the whole system. Known from Fig. 6-7 and Fig. 6-8, the adaptive parameters has larger oscillation than that of Fig. 5-7 and Fig. 5-8. It shows the adaptive parameters can fit the change of initial torques.

D. Further Improvement and Simulation

Seen from Fig. 6-5 and Fig. 6-6, although the initial torque is less than before, it still has large fluctuation. In addition, known from Fig. 6-5, the normal operation torque of link 1 is about 35~75N.m, but its lower initial torque is about -75N.m. So we can set the lower torque limit of link 1 so as to lessen the large fluctuation of initial torque. Of course, the torque of link 2 and the upper limit of link 1 have not any limit so as to guarantee the tracking performance of links. In our simulation, we set the initial torque of link 1 be equal 0 once it is less than 0 in the initial 0.5 second. The simulation results are shown as Fig.7.

Seen from Fig. 7-1 to Fig. 7-2, the tracking speed is accelerated; seen from Fig. 7-5 and Fig. 7-6, the initial torque become smaller. So the further improvements make the system not only have smaller initial torque, but also have faster response speed.

V. Conclusion

This paper establishes the kinematic model of two-freedom-degree manipulator, and the trajectory planning is carried out by using higher order polynomials. Then, utilizing dynamic equation of the manipulator, a backstepping sliding mode control algorithm is designed and improved. The simulation proves that the controller has not only good dynamic quality, but also can effectively weaken the chattering, and quickly track the desired trajectory.

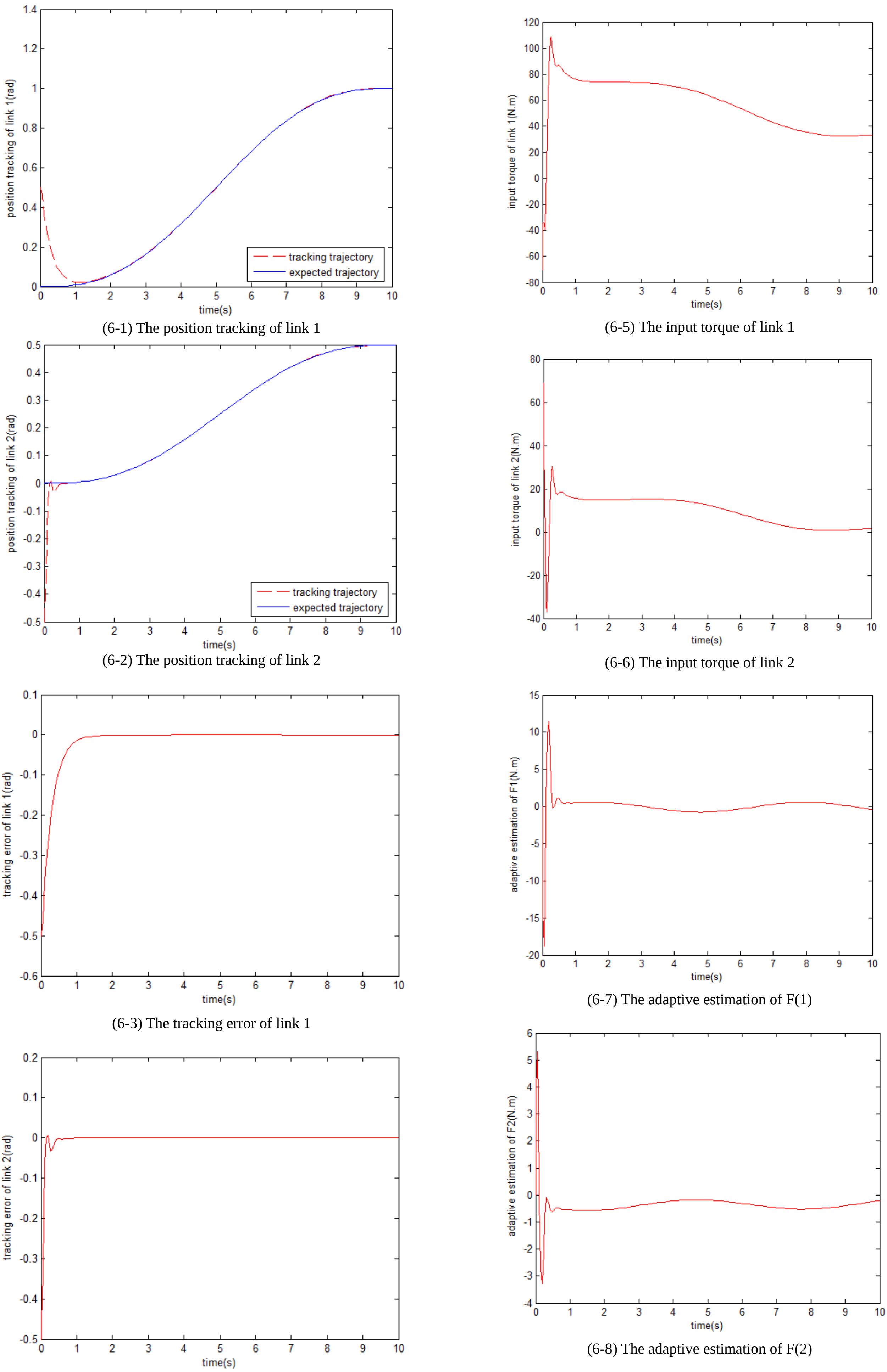

(6-1) The position tracking of link 1

(6-2) The position tracking of link 2

(6-3) The tracking error of link 1

(6-4) The tracking error of link 2

(6-5) The input torque of link 1

(6-6) The input torque of link 2

(6-7) The adaptive estimation of F(1)

(6-8) The adaptive estimation of F(2)

Fig. 6 The improved sliding mode controller using terminal sliding surface

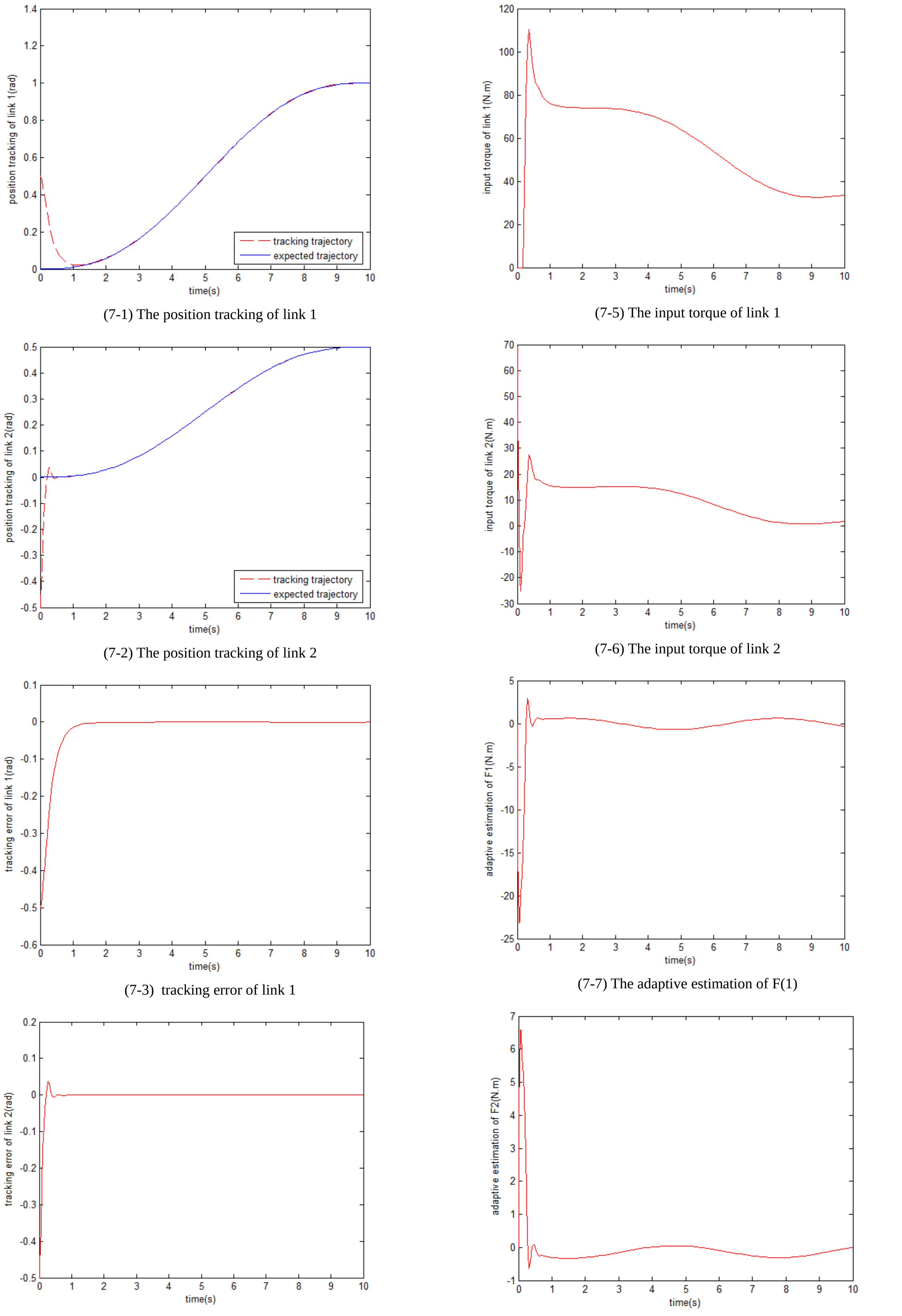

(7-1) The position tracking of link 1

(7-5) The input torque of link 1

(7-2) The position tracking of link 2

(7-6) The input torque of link 2

(7-3) tracking error of link 1

(7-7) The adaptive estimation of F(1)

(7-4) The tracking error of link 2

(7-8) The adaptive estimation of F(2)

Fig. 7 The improved sliding mode controller with the lower torque limit

REFERENCES

[1] Y. W. Zhang, Y. M. Zhang and Y. Q. Huang, “Solving the constrained problem of robot trajectory planning by using higher order polynomial interpolation,” Robot Technique and Application, no. 2, pp. 19-21, 2002.

[2] Z. Shi,Y. Z. Wang and Q. L. Hu, “A polynomial interpolation based particle swarm optimization algorithm for trajectory planning of free-floating space robot,” Journal of Astronautics, vol. 32, no. 7, pp. 1516-1521, 2001.

[3] J. K. Liu and F. C. Sun “Research and development on theory and algorithms of sliding mode control,” Control and Applications, vol. 24, no. 3, pp. 407-417, 2007.

[4] Y. G. Niu, C. W. Yang and X. R. Chen， “Adaptive sliding mode control for robot manipulators based on neural network,” Control and Decision, vo. 16, no. 1, pp. 79-82, 2001.

[5] H. X. Zhang, J. S. Fan, F. Meng and J. F. Huang, “A new double power reaching law for sliding mode control,” Control and Decision, vo. 28, no. 2, pp. 289-293, 2013.

[6] L. P. Xi, Z. L, Chen and X. H. Qi, “Fast sliding mode variable structure control for manipulators with chattering suppression effect,” Electric Machines and Control, vol. 16, no. 7, pp. 97-102, 2012.

[7] H. Mei, “A novel sliding mode variable structure control for robot,” Machine tool ＆ Hydraulics, vol. 37, no. 6, pp. 161-163, 2009.

[8] W. H. Zhang and N. M. Qi, “Neural-network tracking control of space robot based on sliding-mode variable structure,” Control Theory and Application, vol. 28, no. 9, pp. 1141-1144, 2011.

[9] K. W. Dong and X. Zhang, “Sliding mode variable structure control of permanent magnet synchronous machine based on novel reaching law,” Proceeding of CSEE, vol. 28, no. 21, pp. 102-106, 2008.

[10] C. S. Xu, X. J. Sun and G. Y. Cao, “A novel variable structure control for the tracking of robot,” Computer Simulation, vol. 21, no. 7, pp. 114-117, 2004.

[11] J. K. Liu, “MATLAB simulation for sliding mode control,” Tsinghua university press, 2005.

[12] C. Z. Xu, Y. C. Wang, “ Nonsingular Terminal Neural Network Sliding Mode Control for Manipulator Joint Based on Backstepping,” Journal of Mechanical Engineering, vol. 48, no. 23, pp. 36-40, 2012.

[13] Z. X. Cai, “robotics,” Tsinghua university press, 2009.

[14] W. N. Zhai, Y, “W Ge and S. Z. Song. Sliding Mode Control for Robotic Manipulators Based on the Improved Reaching Law,” Information and Control, vol. 43, no. 3, pp. 300-305, 2014.

[15] H. T. Zhang, M. M. Du and W. S. Bu, “Sliding Mode Controller with RBF Neural Network for Manipulator Trajectory Tracking,” IAENG International Journal of Applied Mathematics, vol. 45, no. 4, pp. 334-342, 2015

[16] X. N. Zhang, “Terminal Sliding Mode Control Theory,” Science Press, Beijing, 2011.